

13

Ohmic heating

R. Ruan, X. Ye, P. Chen and C.J. Doona, University of Minnesota and I. Taub, US Army Natick Soldier Center

13.1 Introduction

Over the past two decades, there has been an increasing shift from batch thermal operation towards continuous High Temperature Short Time (HTST) processing of foods. In HTST processes, food is processed continuously through plate or scraped surface heat exchangers at temperatures as high as 140°C. At this temperature, only a few seconds are needed for sterilization, during which the products suffer only a slight quality deterioration. HTST processes rely on rapid convection heat transfer and are thus well suited to liquid foods. They are, however, limited in application to particulates since, for particles more than a couple of millimeters thick, the processing time is insufficient for heat to transfer to the center to give sterility. In ohmic heating processes, foods are made part of an electric circuit through which alternating current flows, causing heat to be generated within the foods due to the electrical resistance of the foods. Therefore, in a liquid-particulate food mixture, if the electrical conductivity of the two phases are comparable, heat could be generated at the same or comparable rate in both phases in ohmic heating. In other conditions, heat can also be generated faster in the particulate than in the liquid. Ohmic methods thus offer a way of processing particulate food at the rate of HTST processes, but without the limitation of conventional HTST on heat transfer to particulates.

13.1.1 History

The concept of ohmic heating of foods is not new. In the nineteenth century, several processes were patented that used electrical current for heating flowable materials. In the early twentieth century, 'electric' pasteurization of milk was achieved by passing¹ milk between parallel plates with a voltage difference

between them, and six states in the United States had commercial electrical pasteurizers in operation.² In the design of McConnel and Olsson,³ frankfurter sandwiches were cooked by passing through electric current for a predetermined time. Schade described a blanching method of preventing the enzymatic discoloration of potato using ohmic heating.¹ It was thought at that time that lethal effects could be attributed to electricity. The technology virtually disappeared in succeeding years apparently due to the lack of suitable inert electrode materials and controls. Since that time, the technology has received limited interest, except for electroconductive thawing.⁴

Within the past two decades, new and improved materials and designs for ohmic heating have become available. The Electricity Council of Great Britain has patented a continuous-flow ohmic heater and licensed the technology to APV Baker.⁵ The particular interest in this technology stems from ongoing food industry interest in aseptic processing of liquid-particulate foods. Conventional aseptic processing systems for particulates rely on heating of the liquid phase which then transfers heat to the solid phase. Ohmic heating apparently offers an attractive alternative because it heats materials through internal heat generation.

13.1.2 Principles

The principles of ohmic heating are very simple as illustrated in Fig. 13.1. Ohmic heating is based on the passage of alternating electrical current (AC) through a body such as a liquid-particulate food system which serves as an electrical resistance in which heat is generated. AC voltage is applied to the electrodes at both ends of the product body. The rate of heating is directly proportional to the square of the electric field strength, E , and the electrical conductivity. The electric field strength can be varied by adjusting the electrode gap or the applied voltage. However, the most important factor is the electrical conductivity of the product and its temperature dependence. If the product has more than one phase such as in the case of a mixture of liquid and particulates, the electrical conductivity of all the phases has to be considered. The electrical conductivity increases with rising temperature, suggesting that ohmic heating becomes more effective as temperature increases, which could theoretically result in runaway heating. A difference in the electrical resistance and its temperature dependence between the two phases can make the heating characteristics of the system very complicated. Since electrical conductivity is influenced by ionic content, it is possible to adjust the electrical conductivity of the product (both phases) with ion (e.g. salts) levels to achieve effective ohmic heating.

In ohmic heating, microbes are thought to be thermally inactivated. Other contributions to the kill mechanism have also been suggested. A mild electroporation mechanism may occur during ohmic heating operating at low frequency (50–60 Hz) which allows electrical charges to build up and form pores across cell walls.

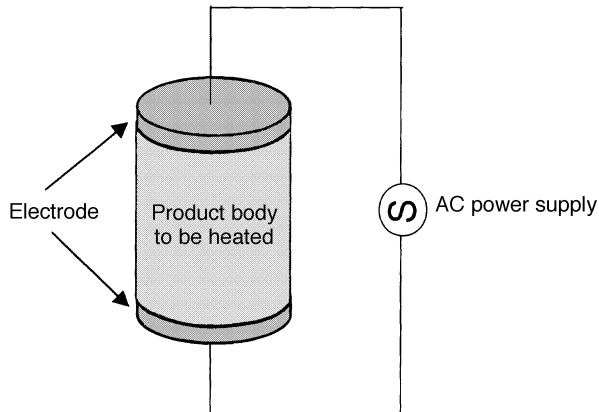


Fig. 13.1 Schematic diagram showing the principle of ohmic heating.

13.1.3 Current status of commercial uses

Currently, at least eighteen ohmic heating operations have been supplied to customers in Europe, Japan, and the United States. The most successful of these systems have been for the processing of whole strawberries and other fruits for yogurt in Japan, and low acid ready-to-eat meals in the United States.⁶ Currently there are two commercial manufacturers of ohmic heating equipment: APV Baker, Ltd., Crawley, UK, and Raztek Corp, Sunnyvale, CA, US.

In the United States, a consortium of 25 partners from industry (food processors, equipment manufacturers, and ingredient suppliers), academia (food science, engineering, microbiology and economics) and government was formed in 1992 to develop products and evaluate the capabilities of the ohmic heating system. A 5 kW pilot-scale continuous-flow ohmic system manufactured by APV Baker, Ltd., Crawley, UK, was evaluated by the consortium at Land-O'Lakes, Arden Hills, Minnesota, from 1992 to 1994. A wide variety of shelf-stable low- and high-acid products, as well as refrigerated extended-shelf-life products were developed. They were found to have texture, color, flavor, and nutrient retention that matched or exceeded those of traditional processing methods such as freezing, retorting, and aseptic processing. The consortium concluded that the technology was viable. In addition to the technical evaluation, an economic study was also initiated. Ohmic operational costs were found to be comparable to those for freezing and retorting of low-acid products.⁷ While the economics and technology appear favorable, there still remains the business risk associated with start-up costs and unknown market potential. For this reason, the consortium did not pursue commercialization of ohmic heating processes.

Although the technological approaches associated with aseptic food processing (i.e., pumps, fillers, heater electrode, etc.) have developed significantly, the identification, control, and validation of all the critical control points required to demonstrate that an ohmically processed multiphase food product has been uniformly rendered commercially sterile have yet to be

generally accepted. Consequently, the Food and Drug Administration (FDA) has no current filing of continuous ohmically processed multiphase food products.

The ohmic heating process has the promise to provide food processors with the opportunity to produce new, high-value-added, shelf-stable products with a quality previously unrealized with current sterilization techniques. Applications that have been developed include aseptic processing of high-value-added ready-prepared meals for storage and distribution at ambient temperature; preheating of food products prior to in-can sterilization; and the hygienic production of high-value-added ready-prepared foods for storage and distribution at chilled temperatures. Ohmic heating can also be used for heating of high-acid food products such as tomato-based sauces prior to hot-filling, with considerable benefits in product quality. Other potential applications include rapid heating of liquid food products, which are difficult to heat by conventional technologies.⁸ Other potential future applications for ohmic heating include blanching, evaporation, dehydration, fermentation, and extraction.

The disadvantages of ohmic heating are associated with its unique electrical heating mechanisms. For example, the heat generation rate may be easily affected by the electrical heterogeneity of the particle, heat channeling, complex coupling between temperature and electrical field distributions, and particle shape and orientation. All these make the process complex and contribute to non-uniformity in temperature, which may be difficult to monitor and control.

13.1.4 Advantages

The advantages of ohmic heating technology claimed in the previous research are summarized as follows.^{5,9}

- Heating food materials by internal heat generation without the limitation of conventional heat transfer and some of the non-uniformity commonly associated with microwave heating due to limited dielectric penetration. Heating takes place volumetrically and the product does not experience a large temperature gradient within itself as it heats.
- Higher temperature in particulates than liquid can be achieved, which is impossible for conventional heating.
- Reducing risks of fouling on heat transfer surface and burning of the food product, resulting in minimal mechanical damage and better nutrients and vitamin retention.
- High energy efficiency because 90% of the electrical energy is converted into heat.
- Optimization of capital investment and product safety as a result of high solids loading capacity.
- Ease of process control with instant switch-on and shut-down.
- Reducing maintenance cost (no moving parts).
- Ambient-temperature storage and distribution when combined with an aseptic filling system.
- A quiet environmentally friendly system.

13.2 Ohmic heating process and equipment

13.2.1 Flow chart and key equipment

Figure 13.2 is a schematic of a continuous flow ohmic heating process. A viscous food product containing particulates enters the continuous-flow ohmic heating system via a feed pump hopper. The product then flows past a series of electrodes in the ohmic column, where it is heated to process temperature. Then the product enters the holding tubes for a fixed time to achieve commercial sterility. Next, the product flows through tubular coolers and into storage tanks, where it is stored until filling and packaging.

Most ohmic heating system configurations consist of three modules: heater assembly, power supply and control panel.

13.2.2 Equipment design

Equipment design is a critical factor that should be considered. The reason for the early failure of ohmic heating to be applied widely on a commercial scale was the absence of inert electrode materials and control equipment accurate enough to keep the temperature within the necessary range and sufficiently robust to withstand the conditions of commercial production. Currently, commercially available designs include electrodes that are located at various positions along the length of the product flow path (in-line field), or those located perpendicular to the flow (cross-field), differing principally in distribution of electric field strength.

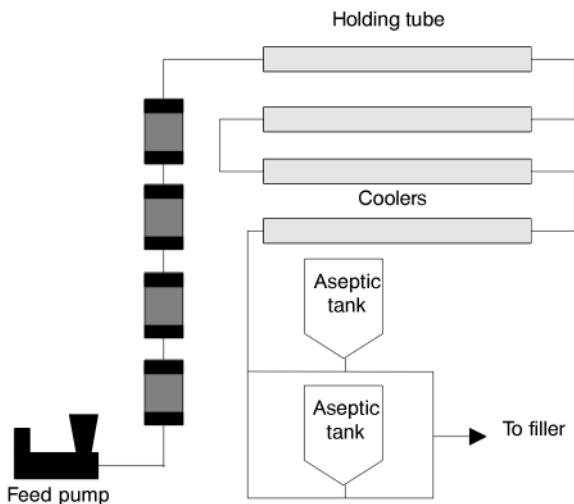


Fig. 13.2 Schematic of a continuous-flow ohmic heating process.

13.2.3 Electrode

Previous designs attempted to use a range of electrode materials from graphite to aluminum or stainless steel. In food processing, high standards of hygienic design are required; electrodes must be carefully designed. In the early designs the electrolytic effect that causes the dissolution of the metallic electrodes was completely neglected, and material technology had not progressed to the stage that a suitable electrode material was available. For recent technologies, such as the APV ohmic process, the use of a food-compatible electrode electrical material and the correct current density has eliminated contamination problems. Other ways to overcome this problem include utilizing high power frequency, since at alternating frequencies above 100 kHz, there is no apparent metal dissolution.

13.2.4 Control

Getchell¹⁰ was the first author to emphasize the importance of controlling the ohmic heating process. Since that time, significant developments in semiconductor technology have taken place, increasing the sophistication of possible control equipment and strategies. In continuous processing, problems can result if a single electrode pair is used to heat food material through a large change in temperature; substantial changes in liquid conductivity and thus in heating rate, may result along the length of the electrode. Multiple sets of electrodes are easier to control. However, Biss *et al.*¹¹ report that pure feedback control was not suitable for the APV Baker ohmic process due to large time constants, and describe the development of a feed-forward control scheme. For feed-forward processes, some idea of the characteristics of the system are needed; control depends as much on process knowledge as on the design of the control loops.

13.2.5 Commercial equipment

A typical commercial ohmic heating system for liquid-particulate mixture is the APV Baker 'ohmic heating' process. The process was originally developed by the UK Electricity Council Research Centre, and was then licensed to APV Baker who have developed it into a commercial system. A diagram of the process is given in Fig. 13.3.

Food is pumped through a vertical pipe containing a series of cylindrical electrodes connected to a 50 Hz three-phase supply. Electric current thus flows through the food in the pipes connecting the electrodes. The food material is rapidly heated to sterilization temperature, then passes to a holding section and finally to an aseptic packaging plant. Unlike most previous techniques, the advantage of ohmic heating in giving rapid sterility is not lost due to the packaging process. The use of multiple electrodes gives a much greater degree of control than is possible in other techniques, together with a uniform electric field in the pipe sections. Specially-developed electrode material is used to eliminate polarization and contamination. The process allows food products containing particulates up to 25 mm to be heated to sterilization temperatures up

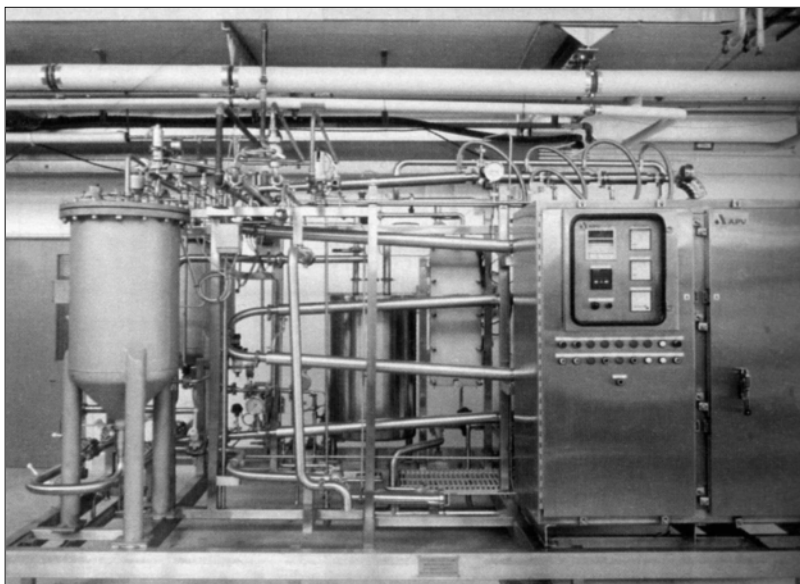


Fig. 13.3 The 5 kW pilot scale ohmic heating system by APV Baker, Ltd. (Courtesy of APV Baker, Ltd.)

to 140°C in less than 90 seconds, after which they are cooled back down to ambient temperatures within 15 minutes. These processing times are significantly shorter than the typical two-hour process cycles for in-can sterilization techniques. The whole process is automatically controlled using a programmable logic controller.

Because all early attempts at commercialization failed due to problems associated with electrode degradation and uneven heating of the product, APV conducted research on several key areas of the technology: electrode arrangement design and establishment of safety standards for such equipment; validation procedures to ensure proper sterilization of food products; and research to ensure the absence of any toxicological effect on food products. These studies resulted in a successful submission in 1991 to the UK Advisory Committee for Novel Foods and Processes for approval of the APV ohmic heating system for the production of ambient stable low-acid, ready-to-eat meals in the United Kingdom. The development also earned the Institute of Food Technologists' 1996 Industrial Achievement Award.

13.3 Monitoring and modeling of ohmic heating

13.3.1 Mathematical modeling

The future utilization of ohmic heating by the industry will depend on development of adequate safety and quality assurance protocols. One crucial

component in understanding the process lies in the development of mathematical models, which can then be used to simulate various effects of critical factors. Two different modeling approaches currently have been published.

De Alwis-Fryer model

De Alwis and Fryer¹² use the solution to Laplace’s equation to calculate heat generation rate together with transient energy balance equations to model a single particulate immersed in a fluid medium without convection. This model has been extended by Zhang and Fryer¹³ to include multiple spheres uniformly distributed on a lattice within a non-convective fluid. A typical situation is illustrated in Fig. 13.4, wherein a cylindrical particle is stationed in the middle of a tube filled with stationary, non-convective fluid. An electric field is applied along the length of the tube.

The electric field or voltage distribution can be developed from Maxwell’s equations, or by combining Ohm’s law and the continuity equation for electrical current:

$$\nabla \cdot (\sigma_i \nabla V) = 0 \tag{13.1}$$

where V = voltage, ∇ = gradient, σ_i = electrical conductivity of phase I which can take on different values for the particles and liquid.

Ignoring convection effects, the heat transfer problem is one of pure conduction with internal energy generation:

$$\nabla \cdot (k_i \nabla T) + \dot{u}_i = \rho_i C_{pi} \frac{\partial T}{\partial t} \tag{13.2}$$

where i again represents the phase, k = thermal conductivity, \dot{u} = specific internal energy generation rate, ρ = density, C_p = specific heat capacity, T = temperature, and t = time.

The external boundary condition is one of convection to the surroundings:

$$-k_{iS} \nabla T \cdot \vec{n} = U(T_{iS} - T_\infty) \tag{13.3}$$

where k_{iS} = thermal conductivity of phase i at surface, \vec{n} = unit normal vector, U = overall heat transfer coefficient, T_{iS} = surface temperature of phase i , and T_∞ = surrounding temperature.

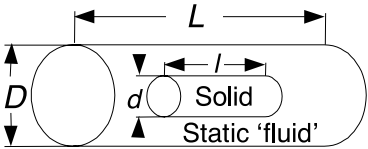


Fig. 13.4 Situation simulated in de Alwis–Fryer model. (Redrawn from Sastry and Salengke.¹⁴)

The internal energy generation term in Equation [13.3] is given by:

$$\dot{u}_i = |\nabla V|^2 \sigma_{0i} (1 + m_i T) \quad [13.4]$$

where ∇V = voltage gradient, σ_{0i} = initial electrical conductivity, m_i = temperature compensation constant, T = temperature.

The system of Equations [13.1–13.4] can be solved by the Galerkin–Crank–Nicolson algorithm, a hybrid-spatially finite element, temporally finite difference scheme.

Sastry-Palaniappan model

Sastry and Palaniappan¹⁵ used circuit analogy to approximate electrical conductivity and thus the heat generation for a static heater with a particle immersed in a well-mixed fluid (assuming infinite convective heat transfer within the fluid). A typical situation is as illustrated in Fig. 13.5.

Sastry¹⁶ extended this approach to a continuous flow ohmic heater for high solid concentration. The effective electrical resistance can be determined using the circuit analogy. The effective resistance of the cell is calculated as:

$$R = R_{fs1} + R_{fs2} + \frac{R_{fp}R_{sp}}{R_{fp} + R_{sp}} \quad [13.5]$$

where the resistance R 's can be calculated from the electrical conductivity and the geometry. The average voltage gradients (∇V) in the liquid and particulate can simply be calculated as:

$$\nabla V = \frac{V}{L} \quad \text{or} \quad \nabla V = \frac{IR}{L} \quad \text{and} \quad I = \frac{V}{R} \quad [13.6]$$

where V is the applied voltage and L the distance between the two electrodes.

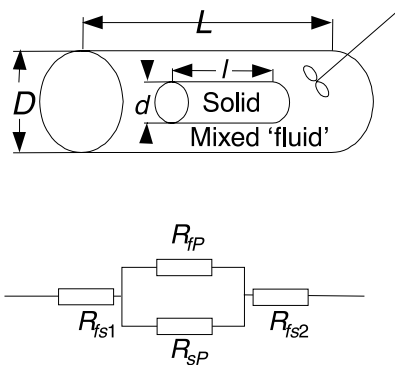


Fig. 13.5 Situation simulated in Sastry–Palaniappan model. Also shown is the circuit analogy. (Redrawn from Sastry and Salengke.¹⁴)

The energy balance on the well-mixed fluid phase is:

$$M_f C_{pf} \frac{dT_f}{dt} = \dot{u}_f v_f + n_p h_{fp} A_p (T_{sSm} - T_f) - UA_w (T_f - T_\infty) \quad [13.7]$$

where the subscript f represents liquid phase and p particulate phase, M_f = mass of fluid, C_p = specific heat capacity, \dot{u}_f = specific internal heat generation rate, v = volume, n_p number of particulates, h_{fp} = liquid-particulate convective heat transfer coefficient, A_p = surface area of one particle, T_{sSm} = mean particulate surface temperature, U = overall heat transfer coefficient to surroundings, A_w = area of heater wall.

The specific internal heat generation rate for the liquid phase \dot{u}_f is given by:

$$\dot{u}_f = |\nabla V|^2 \sigma_{0f} (1 + m_f T) \quad [13.8]$$

The particulate heat according to the conduction heat transfer equation with internal energy generation:

$$\nabla \cdot (k_s \nabla T_s) + \dot{u}_s = \rho_s C_{ps} \frac{dT_s}{dt} \quad [13.9]$$

where

$$\dot{u}_s = |\nabla V|^2 \sigma_{0s} (1 + m_s T_s) \quad [13.10]$$

Temperatures of the two phases are linked by the convective boundary condition:

$$-k \nabla T \cdot \vec{n} |_s = h_{fp} (T_{ss} - T_f) \quad [13.11]$$

This system of equations can be solved by forward differences for the liquid phase, and the Galerkin–Crank–Nicolson method for the solid phase.

For any aseptic process, safety deserves the highest priority. The limitations of these two models and the lack of understanding of the temperature distribution mandate that the conservative approaches be used. Any low-temperature regions that result will extend the process time needed to ensure satisfactory commercial sterility and will make it more likely that other regions of the food will be overcooked. Ohmic heating thus will lose its most attractive advantage. The effects of convection were over simplified in the two models. In reality, the convection heat transfer rate is neither zero nor infinity. A more general model is thus required and convection effects must be included to model the temperature profile.

13.3.2 Experimental and instrumental monitoring

Invasive

Locating the coldest spot within an ohmically heated food system is of significant concern for food engineers and processors. For a high temperature short time thermal process such as heating, the determination of the spatial and temporal

distribution of temperature within the particulate is necessary and important. Not only will it provide information for calculation of lethality and cook value, but it will also provide a guide to mathematical modeling and process control. However, mapping the intra-particle temperature distribution in food material undergoing dynamic ohmic heating is a difficult and complex task. Thermal couples were used for modeling verification and process monitoring. Temperature could only be obtained from selected points and the integrity of the process could be disturbed. Moreover, it is difficult to monitor the temperature of a flowing particle.

Non-invasive: magnetic resonance imaging

Magnetic resonance imaging (MRI) has contributed greatly to a diversity of scientific disciplines in recent years. Applications in the food area have increased significantly as researchers have discovered the power and flexibility of this technique.¹⁷ Food-related MRI research has gone beyond static imaging experiments to experiments involving dynamic processes, diffusion, water mobility, flow, water and oil distribution, and temperature distribution.¹⁷ The major advantages of MRI are that

- it is nondestructive and non-invasive to the material being imaged and the complexity of foods can be probed without disturbing the sensitive balance
- it can provide high spatial resolution
- it can provide diverse information such as proton density (which is related to moisture or fat concentration), internal structure, chemical shift, diffusion, temperature and flow.

Among all the food-related MRI techniques, MRI temperature thermometry is emerging as an attractive and promising temperature mapping method.^{18–22} As pointed out by Hills²³ the true potential of MRI lies not in static structure determination but in non-invasive, real time and dynamic changes as foods are processed, stored, packaged and distributed. When using MRI to map temperature distribution in a dynamic process like ohmic heating, the data acquisition should be as fast as possible so that a real-time measurement can be accomplished. If this temporal resolution cannot be achieved, the measurement will be inaccurate or perhaps even meaningless. Significant progress has been made to apply MRI techniques to mapping temperature distribution of ohmically heated food systems.

Principles and methodology

MRI is an extension of nuclear magnetic resonance (NMR) spectroscopy. Briefly, NMR spectroscopy is based on magnetic behavior of certain nuclei (such as protons in water and fat) in a sample placed in an external bulk magnetic field, and subjected to a radio frequency (RF) pulse. The nucleus of an atom possesses a positive charge, and is considered as spinning about an axis. The spinning of the nucleus generates a magnetic field, which is similar to that

generated by a simple bar magnet, and is termed the nuclear magnetic dipole. When placed in a magnetic field B_0 generated by a permanent magnet, for instance, the nucleus will interact with the applied field via its magnetic dipole, and tend to precess about the direction of the applied field at a specific frequency known as *Larmor* frequency ω , which is proportional to the strength of the applied field B_0 , and governed by the following equation:

$$\omega = \gamma B_0, \quad [13.12]$$

where γ is the magnetogyric ratio, a fundamental property of the nucleus. If a second magnetic field generated by using a radio frequency (RF) coil, for instance, whose frequency exactly matches the *Larmor* frequency ω , is applied as a RF pulse to the nucleus, then resonant absorption of energy occurs. This resonance effect is hence termed nuclear magnetic resonance. In the time following the excitation, the excited spins give up energy and return to their equilibrium state. The energy is released in the form of an RF wave, characterized by its *Larmor* frequency, and discharged into the environment through two mechanisms: spin-lattice and spin-spin relaxation processes, each of which is characterized by a time constant. The time constant for spin-lattice relaxation is called T_1 while for spin-spin relaxation it is called T_2 . In general, T_1 and T_2 can be functions of structure, molecular mobility, temperature, solute and water concentrations, and maybe other physical and chemical properties of the samples. The RF coil also functions as an antenna to receive the RF signals emitted from the nucleus during the relaxation processes, by which the signal decay or relaxation behavior of the spins with characteristic T_1 and T_2 can be recorded.

MRI is based on a function of spatial position of magnetic fields instead of using a uniform static field. If a linear field gradient G_x is superimposed on the main magnetic field along the x direction, the resonance frequency at which the spin precesses is a function of spatial position along x :

$$\omega(x) = \gamma(B_0 + G_x x) \quad [13.13]$$

Transformation of the data then yields not only the magnitude but also spatial information. The same principle can be extended to achieve spatial information in two or three dimensions, which can be used to construct two- or three-dimensional magnetic resonance images. NMR parameters that cause image contrast include nucleus intensity (signal strength), T_1 , T_2 , magnetization transfer rates, self-diffusion coefficients, proton resonance frequency shift, and velocity profiles, and are often termed 'contrast agents'. Using different contrast agents, MR images or maps of NMR parameters and structure of a cross-section of a sample can be obtained.

The fact that many of these contrast agents are a function of temperature makes constructing temperature maps with MRI instruments possible. Among these contrast agents, T_1 , proton resonance frequency shift (PRF), and signal intensity are often the choices for temperature mapping.

T_1 methods

Simply put, the T_1 methods involve the following procedures:

- (1) acquisition of T_1 relaxation data,
- (2) fitting of T_1 values,
- (3) constructing T_1 images,
- (4) experimental calibration between T_1 and temperature, and
- (5) translating T_1 image to temperature image.

Inversion recovery and spin echo imaging sequences are common T_1 imaging methods. Both methods are considered time consuming and unsuitable for monitoring fast changing ohmic heating process. Inversion Recovery-Flip Low Angle Snap Shot (IR-FLASH) is one of the fast pulse sequences for T_1 image acquisition. In one IR-FLASH sequence, magnetization gradually recovers after an inversion pulse; a FLASH image is acquired at a designated time (recovery time) during the recovery. A series of IR-FLASH sequences is repeated, but only with varying recovery time. The images acquired at different recovery times are used to construct the T_1 image by fitting the magnetization values of the images into a single-exponential recovery equation. Total acquisition time for a T_1 image, which usually requires ten or more inversion recovery FLASH images, is about 30 seconds to 1 minute or more. Although this time is much shorter than the two conventional methods mentioned above, it is still long for dynamic food processes like ohmic heating. To shorten the data acquisition time, the pulse sequence can be altered so that we could take a snapshot of the sample at different recovery times during a single recovery without having to repeatedly revert the signal to its original position (negative maximum) for each image. To map T_1 , a series of FLASH images are acquired during magnetization relaxation following a single inversion pulse, almost without delay between two adjacent images.

After T_1 values are computed and a T_1 image is constructed, the next step is to correlate T_1 to temperature and construct a temperature image based on the T_1 image. Calibration between T_1 and temperature is done by measuring the signal intensity of a spot in the MR image where the temperature is measured using fiber optic temperature sensors. This procedure is repeated for several spots and at different temperatures. The relationship between T_1 and temperature (θ) is determined using a linear function as follows

$$T_1 = a + b\theta \quad [13.14]$$

where a and b are constants related to the nature of the material. This calibration should be carried out for each material.

To translate the T_1 data into temperature for a particle, the relationship described by the above equation is applied within the boundary of the sample. This translation procedure can be automated using a computer program that discerns the true signals from background noise and then applies the temperature fit to the true signals only.

PRF method

The temperature sensitivity of the proton resonance frequency (PRF) was first observed by Hindman in 1966.²⁴ The fractional change of water proton resonance frequency ($\Delta\omega/\omega$) with temperature is defined as δ . It is also referred to as proton chemical shift or PRF shift. Mathematically,

$$\frac{\Delta\omega}{\omega} = \delta \cdot \Delta T \quad [13.15]$$

where ΔT is the temperature change. Experimentally, δ has been estimated as $-0.01 \text{ ppm}/^\circ\text{C}$ in water²² and is about the same for ex vivo tissues.²⁵ It is generally assumed that the water PRF shift to lower frequency with higher temperature is caused by rupture, stretching, or a small amount of bending of the hydrogen bonds.^{24,26} This means a reduction in the average degree of association of water molecules, and hence that these shifts are evidence of an increased average shielding constant of the protons. The proton resonance frequency shift imaged at a static field strength B_0 after having undergone a temperature change of ΔT is:

$$\Delta\omega = \delta \cdot \gamma B_0 \cdot \Delta T \quad [13.16]$$

where γ is the gyromagnetic ratio. This frequency change manifests as a phase change when imaged with a gradient-echo sequence having an echo time TE . This phase change $\Delta\Phi$ can be expressed as:

$$\Delta\Phi = \delta \cdot \gamma B_0 \cdot \Delta T \cdot TE \quad [13.17]$$

To use the PRF shift technique to map temperature, a reference phase image is first acquired at a known temperature, and then subtracted from subsequent phase images taken at different temperatures. Temperature maps can therefore be obtained based on the reference temperature and the echo time TE of the image sequence according to equation (13.17) which also indicates that

$$\frac{\Delta\Phi}{\Delta T} = \delta \cdot \gamma B_0 \cdot TE \quad [13.18]$$

The temperature sensitivity of phase images depends on two factors, i.e., the main magnetic field and the echo time of the image sequence. For the same echo time, the temperature sensitivity for a 4.7 Tesla scanner would be three times more than that for a 1.5 Tesla scanner. The actual PRF shift of a material may depart slightly from the apparent value, $-0.01 \text{ ppm}/^\circ\text{C}$. Therefore, the shift is usually regressed to the known temperature in order to find the actual δ .

Ohmic heating of potato, carrot, and beef

Examples

Potato, carrot, and beef were cut into about 2.5 cm^3 cubes. The carrier medium was made up of 50 g/kg starch and 1 g/kg NaCl. An experimental ohmic heating device was constructed of glass. It consisted of a 38 mm dia and 318 mm long

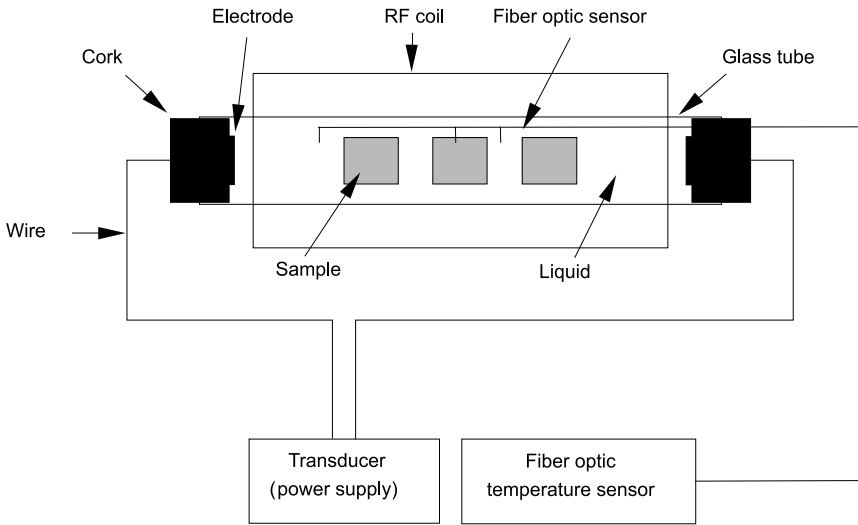


Fig. 13.6 Schematic diagram of the experimental set-up for MR imaging of ohmically heated food particulates.

glass tube with a rubber stopper at each end (Fig. 13.6). A 30 mm diameter stainless still electrode was fixed to each of the stoppers and connected to a transducer corresponding to a 50 Hz AC power supply. A hole was made in one of the stoppers to allow release of pressure built up within the tube during heating. Two fiber optic temperature sensors could be inserted into the tube through this hole, one near the end of the tube and the other in the center. A constant 140 volts was applied.

The MRI images (Fig. 13.7) constructed from these images show that the temperature in the particulates and the corresponding rate of heating the particulates increased with heating time. The increased heating rate was consistent with the rise in electrical conductivity of the particulates with temperature. Wang and Sastry²⁷ reported a higher electrical conductivity for ohmically heated materials compared to unheated raw materials. An increase in heating rate with time was also observed in the liquid phase, reflecting the increase in electrical conductivity with temperature.

These images indicate differences in temperature among different particulates in the same carrier fluids. Beef appeared to heat faster than the others. The differences in heating rate among different materials could be due to differences in electrical conductivity⁹ and/or non-uniformity in the electric field. When two temperature probes were placed in different locations within the heating tube, the observed temperature variation was considerable.

The MR images also show that the temperatures in the center regions of a particulate were higher than in the outer regions, *indicating that the particulate heated intensively and transferred heat to the colder carrier liquid*. Variation in temperature was observed within a particle, probably due to spatial variation in

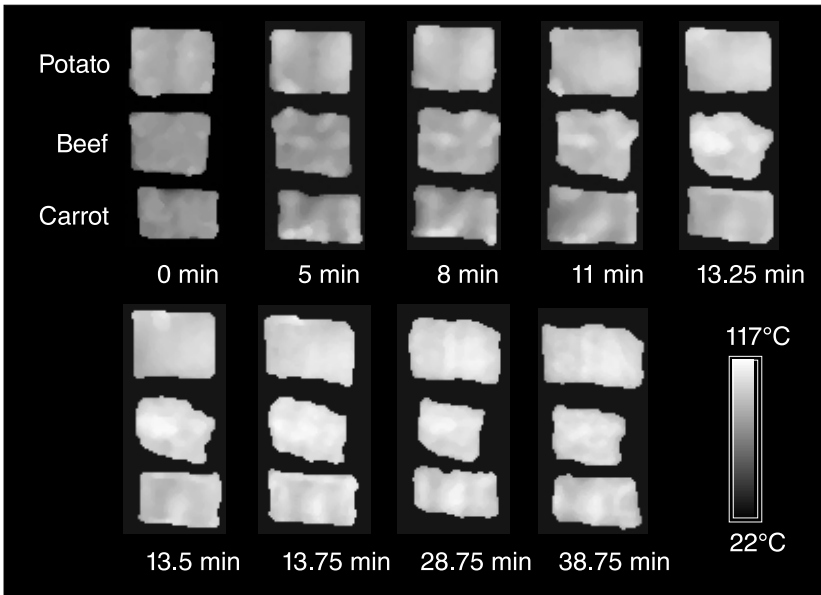


Fig. 13.7 Two-dimensional MR images showing temperature distribution in particulate potato, beef, and carrot undergoing ohmic heating. The numbers indicate the heating time (heating was terminated after 13.75 minutes).

electrical conductivity. Two additional images (Fig. 13.7), taken 28.75 and 38.75 min after heating was terminated show that the heat redistributed within the particulates. These results indicate that, in modeling the ohmic heating process, the generation of heat and associated distribution of temperatures during the heating stage and the redistribution of temperatures during the holding stage all need to be taken into consideration.

Ohmic heating of whey gels

Examples

Whey gels composed of 20% Alacen whey protein powder (New Zealand Milk Products) and 80% distilled deionized water along with NaCl solutions were used as models of a liquid-particulate mixture. Two similar samples of the model system were prepared. It consisted of a 305 mm long hollow cylinder of whey gel and 0.01% NaCl solution. 1.5% NaCl based on the mass of water was also added to the whey gels to adjust their electrical conductivity. A PVC thermal/electrical barrier was inserted into the hollow whey gel to form an insulated passage in the center of the gel cylinder as shown in Fig. 13.8. The model system was configured to resemble electrical circuits and ohmically heated by the application of an AC power supply with a constant voltage of 143 V and frequency of 50 Hz.

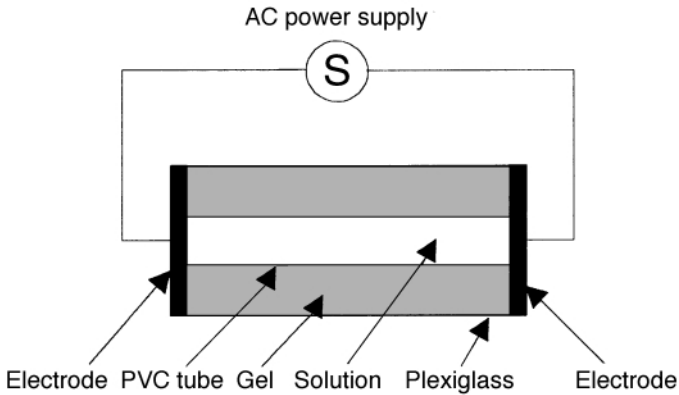


Fig. 13.8 Schematic diagram of the experimental set-up.

An experimental ohmic heating device was constructed (Fig. 13.8). It consisted of a Plexiglas vessel that was 43 mm in inner diameter and a nylon stopper at each end. A 35 mm diameter stainless steel electrode was fixed to each stopper and connected to the power supply. The distance between the two electrodes was 305 mm. A small hole was drilled in one of the stoppers and the Plexiglas vessel to allow the release of pressure build-up during heating. Two fluorescent fiber-optic temperature sensors were inserted through the holes into the whey gel and the solution at the same cross-sectional location that would be scanned to monitor the temperature for calibration. The absolute accuracy of the fiber-optic measurements was $\pm 0.2^\circ\text{C}$. MR susceptibility artifacts were eliminated by using the non-metal temperature sensors.

Figure 13.9 shows the phase change, $\Delta\Phi$, plotted against the temperature change in the whey gel of the sample and the regression line obtained by using linear regression through origin. The slope of the regression line was 0.0567 radians/ $^\circ\text{C}$ and the standard error for the phase was 0.0574 radians. These values correspond to a PRF shift of -0.0098 ppm/ $^\circ\text{C}$ and a temperature uncertainty of $\pm 1.01^\circ\text{C}$. Figure 13.10 is the corresponding graph for the NaCl solution. The PRF shift and the temperature uncertainty in this case were -0.0096 ppm/ $^\circ\text{C}$ and $\pm 2.07^\circ\text{C}$.

Using the phase reference image, phase difference images and the derived PRF shift values, temperature maps of the sample at time 2, 4, and 8 minutes during heating were constructed and are shown in Fig. 13.11. The spatial resolution and temporal resolution were 0.94 mm and 0.64 s respectively. PRF shift was linearly and reversibly proportional to the temperature change. The temperature uncertainties determined were about $\pm 1^\circ\text{C}$ for the whey gel and about $\pm 2^\circ\text{C}$ for the NaCl solution. The temperature maps show that there existed a slight gradient along the radial direction. The existence of this gradient is due to the internal heat generation of ohmic heating process and the radiation heat transfer from the particle surface through the vessel wall to the ambient. Therefore, the cold spots of the particle should be the surface and corners.

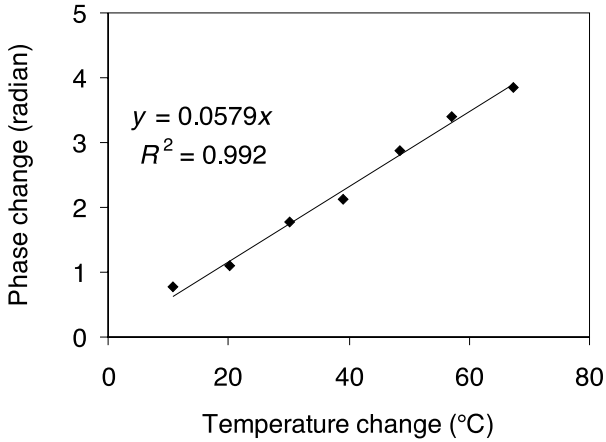


Fig. 13.9 Phase change vs. temperature change and the regression line in the whey gel.

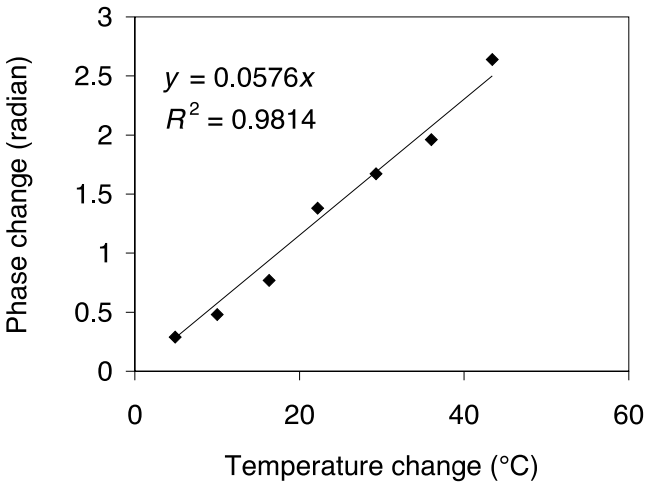


Fig. 13.10 Phase change vs. temperature change and the regression line in the solution.

Intrinsic chemical marker

Kim *et al.*^{28, 29} developed an intrinsic chemical marker approach that was used in conjunction with direct microbiological measurements to map the temperature distribution and calculate lethality for aseptic processing of particulate food. Selecting conditions in which particulates heated faster than the liquid, temperature gradients within the particulates (containing precursor and bacteria) were demonstrated in terms of the concentration of thermally produced compounds (chemical markers) and of the surviving bacterial population.

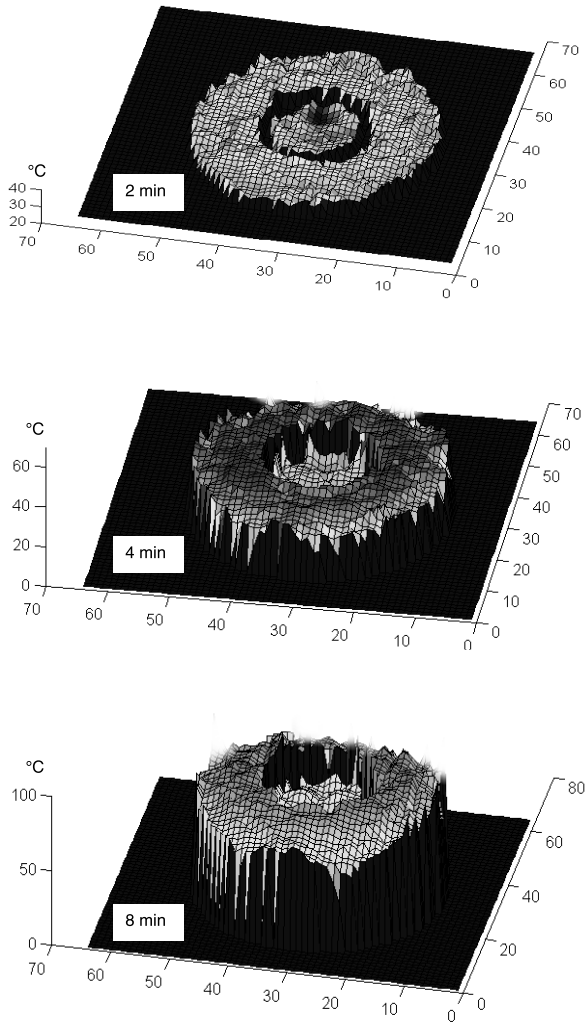


Fig. 13.11 Temperature maps of whey gel during ohmic heating (2, 4, and 8 min).

Chemical markers can be viewed as time-temperature integrators over an HTST domain relevant to thermal processing of foods. At a given temperature, the concentration of a suitable chemical marker should be directly proportional to the log reduction in bacterial population.

Measuring the yields of intrinsic chemical markers produced in hollow whey cylinders subjected to ohmic heating provided another method for mapping the temperature distribution generated in the sample that produced results remarkably consistent with those found using MRI. The experimental conditions were similar in each case. For the marker method, a 25.2 cm hollow cylinder of whey filled the

entire length of the ohmic cell. In addition to containing 1.5% NaCl, the 20% whey preparation also contained 0.4 M ribose, the precursor for chemical marker M-2. The initial applied voltage was 140 V. To monitor the temperature during heating, individual fiber optic probes were inserted through the top of the ohmic cell to a depth of approximately 11 cm in each of the particulate and solution phases. After the ohmic heating, the whey cylinder was cooled and sectioned, then M-2 was harvested from distinct locations of the sample. The yield of M-2 was analyzed at its absorption maximum of 285 nm using HPLC/UV-Vis.

Three primary differences distinguish the MRI and chemical marker experiments. First, MRI measurements are made during heating, and marker yields are determined post-processing. Second, the ohmic cell is oriented *horizontally* for MRI analysis, but *vertically* for marker experiments. Third, the marker experiments were controlled to maintain constant high sample temperatures by gradually reducing the applied voltage during the heating process. In conditions in which the temperature of the whey was maintained constant at a temperature of 94°C (Fig. 13.12a) generated uniform M-2 yields along the long axis of the whey cylinder sample (Fig. 13.12b). The extent of conversion of ribose to M-2 ranged from 20–25% of the maximum attainable yield. The slight trend of increasing marker yield from the bottom to top of the whey sample represents stratification in which heat rises from the lower regions to heat the upper regions faster. Although MRI methods have excellent resolution along the radial axis, measuring marker yields, which are not constrained to a single slice, conveniently complement the MRI results by determining the temperature along the long axis of the sample. In a similar experiment, the temperature-time profile for each phase (Fig. 13.12c) demonstrates that the high electrical conductivity whey cylinder heats faster than the low conductivity central solution. This type of heating pattern has been successfully mathematically modeled using the Unit Cell Model.³⁰

Temperature-sensitive liquid crystal

Sastry and Li³¹ reported a method that used temperature-sensitive liquid crystal sheets to monitor temperature of particulate flowing in a continuous ohmic heater. Transparent solid particles were suspended in fluid and a liquid crystal-coated sheet changed color from black to red to green to blue to black over a specified range of temperature. The sheet was placed parallel to the electric field so the interference with the electric field was minimal and the entire temperature profile inside a solid object could be visualized. This method provided useful information for the temperature distribution and for the model verification.

13.4 Major challenges and needs for future research and development

Three major challenges hindering the commercialization of ohmic heating processing are:

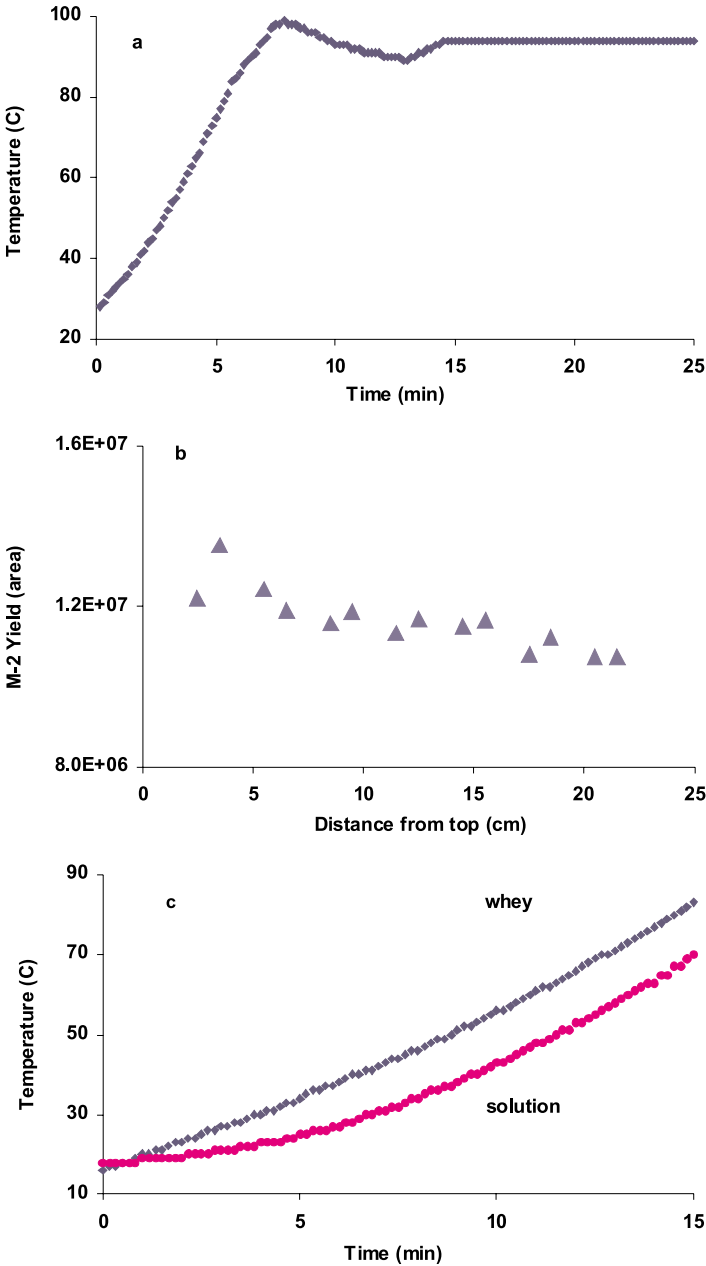


Fig. 13.12 Ohmic heating of whey gel and NaCl solution in the chemical marker experiment: (a) temperature of whey gel as a function of ohmic heating time, (b) chemical marker yield in whey under constant temperature condition as shown in a, (c) effect of electrical conductivity on heating of whey and solution.

1. Lack of a complete model that takes into account differences in electrical conductivity between the liquid and solid phases and the responses of the two phases to temperature changes, which affect relative heating rates and distribution.
2. Lack of data concerning critical factors affecting heating, including residence time, orientations, loading levels, etc.
3. Lack of applicable temperature validating techniques for locating cold/hot spots.

These issues are in part being addressed, as the preceding sections indicate.

13.4.1 Develop reliable, predictive models of ohmic heating patterns

Modeling ohmic heating is difficult owing to the unique character of this mode of heating, which requires much understanding of the critical factors. The ohmic heating rate is critically dependent on the electrical conductivity of the foods being processed for which only limited information is available. If the electrical conductivities of the liquid and particulate phases are the same, the mixture can be heated rapidly and uniformly to a high temperature irrespective of particle size. If the conductivity of the particulate is higher than the liquid, then it heats faster and transfers heat to the liquid, which has advantages for ensuring process adequacy.⁹ Nevertheless, possible heat channeling, which could cause coupling between temperature and electrical field distributions as well as sensitivity to process parameters, e.g. particle shape and orientation, could contribute to the complexity of the process. To ensure sterilization, the heating behavior of the food must be understood, so process reliability and safety could be demonstrated. Kim et al⁹ showed that monitoring the temperature at the entrance and exit of the holding tube could provide such assurances.

Mathematical modeling allows insight into the heating behavior of the process. Spatial and temporal temperature distribution obtained from a reliable mathematical model that incorporates the critical factors can provide information for the calculation of lethality and cook value. It will also save time and money for validation experiments, process and product design. Modeling of a continuous ohmic heating process is difficult, because a number of different physical phenomena occur during the heating process. The verification of the predictions by any model will be limited to selected regions within the system. These limitations require that direct or indirect measurements of the temperature within the product and its constituents be made when establishing a process. Using appropriate conservative assumptions can compensate for some of these limitations (at the expense of the product quality). A general and reliable model is needed.

13.4.2 Develop product specifications and process parameters for specific products

Particulates are the centerpiece around which an ohmic heating formulation is built. Contrary to conventional heating, in which we expect little difference in heat transfer due to changes in particle orientation, the heating pattern of an

ohmically-heated food system would be influenced by particle orientation. De Alwis *et al.*¹² showed the heating of identically-shaped potato particles differed depending on whether the particles were aligned parallel or perpendicular to the electric field. De Alwis *et al.* explained that this difference is due to changes in the electric field, but it also reflects a change in the equivalent resistance of the overall circuit. When both the heating and cooling stages are considered, a practical limitation on particle size and shape might be expected. Cooling of particulates will always be thermal conduction controlled. The center of large particles may cool too slowly and thus become overprocessed during prolonged cooling. Consequently, particulate size is limited to 1 in³. Various combinations of particulates can be successfully processed when accompanied by suitable product and process control. Optimizing the combination will result in excellent particulate texture through uniform heating.

The liquid phase must also be optimized. Viscosity should be determined at various temperatures to assure adequate suspension of particulates and to facilitate liquid/particle interface heat transfer.

Overall product specification is important in determining how much lethal treatment is delivered during the process. Critical factors include particle size, shape, and orientation, viscosity, pH, specific heat, thermal conductivity, solid-liquid ration, and electrical conductivity.

Process design, a complete description of the critical processing conditions, is also important in ensuring lethality and optimizing quality. It should include batch formulation procedures, initial temperature, flow rate or particle residence time, exit temperature, and solid loading levels. These parameters will be specific for individual systems and formulations, and their impact on heating behavior needs to be understood.

13.4.3 Develop real-time temperature monitoring techniques for locating slowest heating regions

Pioneers of ohmic heating research have documented that a particle does not heat uniformly during an ohmic heating process because of the non-uniform nature of the electric field and the differences in the physical properties of the food materials.³² As with any other thermal process, it is important to have information on the temperature-time history of the coldest point within the liquid-particulate system undergoing ohmic heating.

It is assumed that the agitation of a continuous processing system minimizes any disparity among the temperature profiles of the particulates. However, there is no sufficient published evidence to indicate what the temperature is within a particle and how the temperature profile changes during a continuous process. It is clear that, for a particle with a homogeneous electrical conductivity greater than that of the liquid, the particle heats faster than the liquid phase, its coldest spot occurs at its surface¹ and the liquid is colder than the particle.⁹ The location of the slowest heating part of the system is especially important, because its thermal lethality must be ensured. This is the key factor to determine the processing time.

Conventional tools such as thermocouples and fiber optic probes are invasive when used to measure ohmic-heated food systems. A non-destructive and non-invasive technique that can be used to monitor the spatial distribution of temperature is important for understanding and controlling ohmic heating. The MRI temperature mapping technique described here is essential for model development and the validation of the novel ohmic heating process. There is a need to further improve the MRI technique, using it to collect data under various product specifications and processing conditions, and to use it to validate mathematical models.

13.5 References

1. SCHADE AL, Prevention of enzymatic discoloration of potatoes, 1951, US patent 2,569,075.
2. SASTRY SK, PALANIAPPAN S, Ohmic heating of liquid-particle mixtures, *Fd Technol.*, 1992, **46**, 64–7.
3. MCCONNELL SV, OLSSON RP, Wiener vending machine, 1938, US Patent 2,139,690.
4. DE ALWIS AAP, FRYER PJ, The use of direct resistance heating in the food industry, *J Fd Eng.* 1990, **11**, 3–27.
5. SKUDDER PJ, Ohmic heating: new alternative for aseptic processing of viscous foods, *Food Engineering*, 1988, **60**, 99–101.
6. ANON., Ohmic heating garners 1996 industrial achievement award, *Fd Technol.*, 1996, **20**, 114–15.
7. ZOLTAI P, SWEARINGEN P, Product development considerations for ohmic processing, *Fd Technol.*, 1996, **50**, 263–6.
8. PARROTT DL, Use of ohmic heating for aseptic processing of food particulates, *Fd Technol.*, 1992, **46**, 68–72.
9. KIM HJ, CHOI YM, YANG TCS, TAUB IA, TEMPEST P, SKUDDER PJ, TUCKER G, PARROTT DL, Validation of ohmic heating for quality enhancement of food products, *Fd Technol.*, 1996, 253–61.
10. GETCHELL BE, Electric pasteurization of milk, *Agric. Engng.*, 1935, **16**, 408.
11. BISS CH, COOMBES SA, SKUDDER PJ, The development and application of ohmic heating for the continuous heating of particulate foodstuffs, *Engineering innovation in the food industry*, Bath, UK, Institution of Chemical Engineers, 1987, 11–20.
12. DE ALWIS AAP, FRYER PJ, A finite element analysis of heat generation and transfer during ohmic heating of foods, *Chem. Eng. Sci.*, 1990, **45**, 1547–59.
13. ZHANG L, FRYER PJ, Models for the electrical heating of solid-liquid food mixtures, *Chem. Eng. Sci.*, 1993, **48**, 633–43.
14. SASTRY SK, SALENGKE S, Ohmic heating of solid-liquid mixtures: a comparison of mathematical models under worst-case heating conditions, *Journal of Food Process Engineering*, 1998, **21**, 441–58.

15. SASTRY SK, PALANIAPPAN S, Mathematical modeling and experimental studies on ohmic heating of liquid-particle mixtures in a static heater, *Journal of Food Process Engineering*, 1992, **15**, 241–61.
16. SASTRY SK, Application of ohmic heating to continuous sterilization of food, *Indian Food Industry*, 1992, **11**, 28–30.
17. RUAN RR, CHEN PL, *Water in foods and biological materials: A nuclear magnetic resonance approach*, Lanaster: Technomic Publishing Co., 1998.
18. CHANG K, RUAN RR, CHEN PL, FULCHER RG, BASTIAN E, Moisture, fat and temperature mapping of cheese block during cooling using MRI, Paper No. 956535, 1995, presented at ASAE Summer meeting.
19. HULBERT GJ, LITCHFIELD JB, SCHMIDT SJ, Temperature mapping in carrot using T_1 weighted magnetic resonance imaging, *J. Fd Sci.*, 1995, **60**, 780–5.
20. RUAN RR, LONG Z, CHANG K, CHEN PL, TAUB IA, Glass transition temperature mapping using magnetic resonance imaging, *Transactions of the ASAE*, 1999, **42**, 1055–9.
21. SUN X, LITCHFIELD JB, SCHMIDT SJ, Temperature mapping in a model food gel using magnetic resonance imaging, *J. Fd Sci.*, 1993, **68**, 168–72, 181.
22. SUN X, SCHMIDT SJ, LITCHFIELD JB, Temperature mapping in a potato using half Fourier transform MRI of diffusion, *J. Fd Proc. Engr.*, 1994, **17**, 423–37.
23. HILLS B, Food processing: an MRI perspective, *Trends in Food Science & Technology*, **6**, 111–17.
24. HINDMAN JC, Proton resonance shift of water in the gas and liquid states, *J. Chem. Phys.*, 1966, **44**, 4582–92.
25. PETERS RD, HINKS RS, HENKELMAN RM, Heat-source orientation and geometry dependence in proton-resonance frequency shift magnetic resonance thermometry, *Magn. Reson. Med.*, 1999, **41**, 909–18.
26. MULLER N, REITER RC, Temperature dependence of chemical shifts of protons in hydrogen bonds, *J. Chem. Phys.*, 1965, **42**, 3265–9.
27. WANG WC, SASTRY SK, Changes in electrical conductivity of selected vegetable stuffs during multi-thermal treatments, IFT Annual Meeting 1995, Anaheim, CA, 1995.
28. KIM H-J, TAUB IA, Intrinsic chemical markers for aseptic processing of particulate foods, *Food Technol.*, 1993, 91–9.
29. KIM HJ, CHOI YM, HESKITT B, SASTRY SK, LI Q, Chemical and microbiological investigation of ohmic heating of particulate foods using a static ohmic heater. IFT Annual Meeting, Anaheim, CA, 1995.
30. DOONA CJ, POULIN N, SEGARS R, TAUB IA, KANDLIKAR S, RUAN R, YE X, Modeling ohmically-heated whey protein gel circuits, IFT Annual Meeting, Chicago, IL, 2000.
31. SASTRY SK, LI Q, Modeling the ohmic heating of foods, *Food Technol.*, 1996, **50**, 246–8.
32. FRYER PJ, DE ALWIS AAP, KOURY E, STAPLEY AGF, ZHANG L, Ohmic processing of solid-liquid mixtures: heat generation and convection effects, *Journal of Food Engineering*, 1993, **18**, 101–25.